The paper was published in the proceedings of the 11th International Conference on Physical Modelling in Geotechnics (ICPMG2026) and was edited by Ioannis Anastasopoulos. The conference was held from June 8th to June 12th 2026 in Zurich, Switzerland.

Proceedings of the 11th ICPMG 2026
11th International Conference on Physical Modelling in Geotechnics
8-12 June 2026, Zurich, Switzerland

Numerical investigation for soil-monopile interaction of a model test under lateral cyclic loading

M.F. Erener
Ege University, Izmir, Türkiye, fahrettinerener@gmail.com

C.T. Akdag
Technische Universität Berlin, Berlin, Germany, akdag@tu-berlin.de

D.S. Erdogan, T. Tufan Erener
Ege University, Izmir, Türkiye, devrim.erdogan@ege.edu.tr, tugce.tufan.erener@ege.edu.tr

ABSTRACT: In this study, a three-dimensional numerical investigation was conducted to evaluate the cyclic lateral behaviour of a model-scale monopile embedded in saturated medium-dense sand. The finite element model was developed in OpenSeesPL using the Pressure-Dependent MultiYield02 (PDMY02) constitutive model with an explicit representation of the soil-pile interface. The model was validated against 1g model test results, and comparisons were made in terms of pile head displacement accumulation, deformation and rotation profiles along the pile, and soil-pile interaction behaviour during the first 50 loading cycles. The numerical results reproduce the main characteristics of the experimental response. In addition, the computed p-y relationships indicate that API (2014) curves tend to overpredict soil reaction at intermediate depths and do not capture the cycle-dependent reduction in soil resistance observed in the simulations.

1 INTRODUCTION

Monopile foundations are the most widely adopted foundation system for offshore wind turbines. With the increasing trend toward larger diameters and deeper water installations, reliable prediction of their cyclic lateral response has become a critical design issue due to nonlinear soil behaviour, deformation accumulation, and stiffness degradation under cyclic loading.

Although numerous experimental and numerical studies have investigated cyclic lateral loading of piles (e.g., Long and Vanneste, 1994; Lin and Liao, 1999; Verdure et al., 2003), available datasets are often limited in terms of pile diameter, stress level, or number of loading cycles. In parallel, conventional design approaches using p-y curves, may not fully capture the soil reaction under cyclic loading conditions and displacement accumulation observed in model tests and field conditions.

The objective of the present study is to establish and evaluate a three-dimensional finite element modelling (3D FEM) approach for simulating the cyclic lateral response of a monopile foundation at model scale. This study focuses on constitutive model parameter selection, interface representation, and FEM configuration required to reproduce experimentally obtained pile behaviour. For this purpose, the developed FEM is validated against an existing physical model test reported by Akdag et al. (2023). The comparison aims to assess whether the adopted modelling methodology can reliably capture main characteristics of the monopile lateral response such as pile head displacement accumulation, deformation profile along the pile, and cyclic soil-pile interaction behaviour.

Through this modelling approach, the study aims to provide insight into the applicability and limitations of the adopted numerical framework for simulating the response of a model-scale monopile subjected to unidirectional horizontal cyclic loading.

2 EXPERIMENTAL STUDY

The experimental data used for numerical validation in this study were obtained from the 1g monopile tests conducted by Akdag et al. (2023). The experimental program was designed to represent the lateral response of a large-diameter monopile foundation (D=9 m, L≈50m, L/D≈5.55) supporting an 8 MW offshore wind turbine.

The model monopile consisted of a tubular steel pile with an outer diameter D=0.194 m, wall thickness t=3.2 mm, and embedded length L_e=3.20 m. The total pile length was 3.45 m, with 0.25 m extending above the ground surface for load application. The steel elastic modulus was E = 210 GPa. The geometric slenderness of the model pile (L/D≈16.5) differs from the prototype; however, similarity considerations in terms of pile behaviour (rigid, semi-rigid or flexible) are discussed separately in the scaling section.

The experiments were conducted in a rigid test pit with internal dimensions of 4.0 m (longitudinal direction), 3.0 m (transverse direction), and 4.0 m (vertical depth). The pile was positioned centrally within the container. A cross-sectional view of the experimental setup and instrumentation layout is shown in Figure 1.

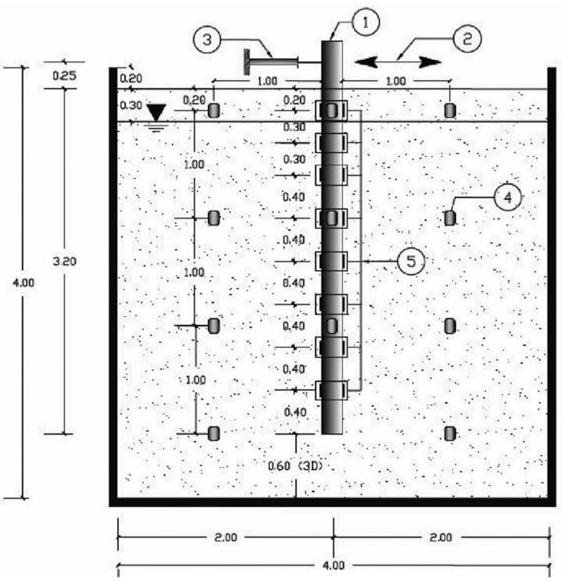

Figure 1. Experimental setup (Akdag et al., 2023).

The soil used in the tests was Cottbuser sand, classified as poorly graded sand (SP). The sand deposit was prepared in layers and each layer was dynamically compacted to achieve a target relative density of D_r=64%, corresponding to medium-dense relative density. The soil depth was kept at 3.8m. Following placement, the sand mass was saturated to reproduce undrained loading conditions relevant for offshore foundations. The index properties of Cottbuser sand are summarized in Table 1.

Table 1. Index properties of Cottbuser sand used in the experiment.

Soil property	Value
Average dry density, ρ_d (g/cm^3)	1.64
Maximum dry density, ρ_{dmax} (g/cm^3)	1.76
Minimum dry density, ρ_{dmin} (g/cm^3)	1.45
Average void ratio, e	0.62
Maximum void ratio, e_{max}	0.82
Minimum void ratio, e_{min}	0.50
Specific density, ρ_s (g/cm^3)	2.65
Coefficient of curvature, C_c	1.03
Coefficient of uniformity, C_u	2.90
D_{50} (mm)	0.67

Lateral cyclic loading was applied at the pile head using a hydraulic actuator under load-controlled sinusoidal loading with a maximum amplitude of 15 kN (approximately 15% of the ultimate monotonic lateral capacity) and a frequency of 0.20 Hz. A total of 12,000 one-way cycles were performed, while the first 50 cycles were considered for the present numerical validation.

Pile head displacements were measured using displacement transducers to capture cyclic accumulation, and strain gauges installed along the pile surface were used to obtain strain and derive bending moments along to pile in order to estimate lateral deformation of pile during the applied number of cycles. The measured head displacement and strain data along the pile serve as the basis for validating the finite element simulations presented in this study.

2.1 Scaling considerations

The physical model tests were conducted under 1g conditions. In 1g small-scale modelling, strict similitude of stresses cannot be achieved; therefore, scaling cannot rely solely on geometric similarity. Instead, the objective is to reproduce the dominant response mechanisms governing the prototype behaviour within laboratory constraints.

In the model test study, scaling considerations addressed both geometric similitude and the expected lateral response of the pile. Cross-sectional dimensions were defined following the scaling approach proposed by Wood (2004). In addition to geometric relationships, the behavioural classification of the pile (rigid, semi-rigid, or flexible) under lateral loading was evaluated using two established criteria. First, the approach of Davisson (1970) was applied by examining the ratio of the embedded length L_e to the elastic length L_{el}, where L_{el} depends on the pile bending stiffness E_pI_p and the initial modulus of subgrade reaction, k. Second, the dimensionless pile relative stiffness parameter K_r, introduced by Poulos (1982), was assessed together with the aspect ratio L/D to characterize the lateral behaviour; this stiffness-based classification has also been adopted in offshore monopile studies (e.g., Abadie et al., 2019).

Based on these scaling considerations, it was concluded that the response of the scaled monopile can represent that of the intended prototype monopile. The 1g large-scale model test was conducted on an open-ended steel pile with D=0.194 m, D/t=60.53 and L=3.20 m. This configuration represents prototype monopiles with diameters of 8-10m, D/t≈75, and embedment lengths of 45-50 m, corresponding to aspect ratios of approximately 5-6.25 under the adopted scaling relationship. The details of the scaling approach can be found in the study by Akdag et al. (2023) and Akdag&Rackwitz (2023).

3 FINITE ELEMENT MODEL

3.1 Numerical model

The numerical model was developed in OpenSeesPL platform, which is developed on the open-source OpenSees (Open System for Earthquake Engineering Simulation) framework widely used for structural and geotechnical simulations under dynamic loading conditions (Mazzoni et al., 2006, Lu et al., 2011).

The model domain extends 3.8 m in depth, 4.0 m in the loading direction (x-direction), and 2.0 m in the transverse direction (y-direction). A half-model configuration was adopted in the transverse direction by utilizing geometric symmetry with respect to the loading application. Accordingly, the 7.5 kN lateral load was applied at the pile head, corresponding to half of the 15 kN load used in the experimental study.

The soil domain was represented using 8-noded BrickUP (u-p) elements, which account for the coupled response of the soil skeleton and pore fluid based on Biot’s formulation. In this formulation, pore water pressure is treated as an independent degree of freedom, and excess pore pressure generation and dissipation are governed by the specified permeability and the applied loading rate. In total, the model consists of 1428 soil elements and 1804 soil nodes.

The monopile was modelled using beam elements connected to the surrounding soil nodes through rigid links located at a radial distance equal to the pile radius. The pile-rigid link system comprises 183 beam and rigid link elements and 184 associated nodes.

The soil-pile interface was represented by introducing a three-dimensional interface zone around the pile. Earlier studies on finite element modelling of monopiles using OpenSeesPL (e.g., Corciulo et al., 2017; Kementzetzidis, 2019) commonly applied reduction factors to the peak friction angle and shear modulus within the interface zone to account for the softer and potentially disturbed behaviour at the soil-pile contact. In these studies, an interface thickness of approximately 4% of the pile diameter was recommended, primarily for large-diameter or prototype-scale monopiles.

In the present study, however, the interface properties were determined within a parameter estimation framework based on available experimental results. Considering that the current analysis focuses on a small-diameter model-scale monopile (D = 0.194 m), an interface thickness of 10%D (0.0194 m) was adopted. It should be noted that this thickness is defined specifically for the model-scale simulations and is not recommended to be directly extrapolated to prototype-scale dimensions.

The finite element mesh was defined with local refinement in regions where stress concentrations were anticipated. In particular, mesh refinement was introduced within a circular region centred at the pile axis and extending 3D radially (i.e., a 6D diameter zone as shown in Figure 2), similar to the modelling approach adopted by Akdag & Rackwitz (2023). Additionally, the vertical element size was reduced in the vicinity of the pile.

Within this modelling approach, the pile material properties and cross-sectional characteristics used in the numerical analysis were obtained from Akdag et al (2023). The constitutive model parameters for both the soil and the interface materials were selected based on the parameter estimation framework described in following sections. The overall configuration of the finite element model is illustrated in Figure 2.

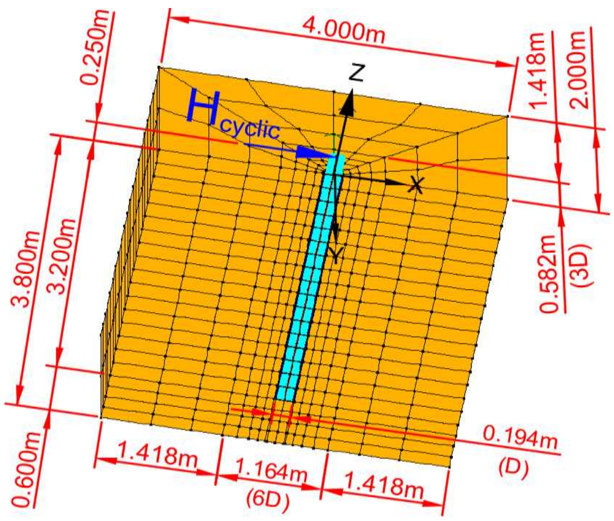

Figure 2. Finite element model with soil domain dimensions, coordinate system and loading configuration.

3.2 Constitutive model

The Pressure-DependentMulti-Yield02 (PDMY02) constitutive model was adopted in this study to represent the cyclic behaviour of sand under undrained loading conditions in the numerical simulations. This model is particularly suitable for capturing cyclic mobility effects since it incorporates pressure-dependent yielding and employs contraction and dilation rules that enable realistic simulation of stiffness degradation, plastic strain accumulation, and excess pore water pressure generation under cyclic loading (Elgamal et al., 2002; Yang et al., 2003). A defining feature of PDMY02 is its non-associative volumetric flow mechanism, implemented through separate contraction and dilation rules, which directly govern whether pore pressure tends to build up or be relieved during loading. Further theoretical background on the constitutive model formulation and finite element implementation is provided by Khosravifar (2012).

In this framework, the contraction parameters (c_1, c_2, c_3) control the rate of contractive volumetric tendency and thus the buildup of excess pore pressure, while the dilation parameters (d_1, d_2, d_3) regulate the onset and intensity of dilative behaviour, influencing the cycle-dependent strain accumulation. It should be noted that careful selection of the contraction and dilation parameters is required to ensure that the numerical response remains consistent with experimentally observed trends under undrained cyclic loading.

3.3 Estimation of model parameters

The suitability of the selected constitutive model parameters plays a critical role in numerical simulations. In this study, the model parameters of PDMY02 for the soil and soil-pile interface elements were determined through a parameter estimation approach.

Due to the absence of laboratory test data for undrained behaviour under cyclic loading and sand-steel interface behaviour of the Cottbuser sand used in the model test, experimental datasets from Vargas et al. (2024) and Zhang et al. (2021) were adopted. Available index properties of Ottawa F-65 sand (El Ghoraiby et al., 2019; Vargas et al., 2024) and Fujian sand (Zhang et al., 2021) are given in Table 2 and Table 3.

Table 2. Index properties of Ottawa F-65 sand (El Ghoraiby et al., 2019; Vargas et al., 2024).

Soil property	Value
Maximum dry density, ρ_{dmax} (g/cm^3)	1.77
Minimum dry density, ρ_{dmin} (g/cm^3)	1.50
Maximum void ratio, e_{max}	0.76
Minimum void ratio, e_{min}	0.50
Specific density, ρ_s (g/cm^3)	2.65
Coefficient of curvature, C_c	0.95
Coefficient of uniformity, C_u	1.73
D_{50} (mm)	0.20

Table 3. Index properties of Fujian sand (Zhang et al., 2021).

Soil property	Value
Maximum void ratio, e_{max}	0.85
Minimum void ratio, e_{min}	0.52
Specific density, ρ_s (g/cm^3)	2.65
Coefficient of curvature, C_c	0.95
Coefficient of uniformity, C_u	1.54
D_{50} (mm)	0.34

3.3.1 Parameter selection for soil element

A single element simulation was performed based on cyclic direct simple shear (CDSS) test results reported by Vargas et al. (2024). The relative density of test specimen was reported as D_r=60-65%, which is consistent with the Cottbuser sand considered in the model test. In the CDSS test, cyclic shear stress with an amplitude of 18 kPa and a loading frequency of 0.1 Hz was applied under an effective confinement of 100 kPa over 16 loading cycles.

In the present study, the numerical model for single element simulation was established using 8-noded BrickUP elements with PDMY02 constitutive model and appropriate boundary conditions to represent the direct simple shear conditions. Accordingly, selected model parameters were evaluated by comparing the numerical outputs with the experimental results in terms of stress-strain relationship, effective stress path and development of excess pore pressure by loading cycles.

It should be emphasized that the selected constitutive model parameters are valid for the considered relative density (D_r=60-65%) and were derived to reproduce the cyclic response at this density level. As illustrated in Figure 3, a reasonable agreement is observed between the experimental and numerical soil responses. This indicated that the adopted parameters provide an adequate representation of the soil behaviour within the scope of the present modelling study. Model parameters for soil elements are given in Table 4.

Table 4. Selected PDMY02 constitutive model parameters for the soil element corresponding to D_r=60-65%.

Parameter	Value	Unit
Small strain shear modulus, (G)	112.5	MPa
Small strain bulk modulus, (K)	237.5	MPa
Reference pressure, (σ'_{ref})	100	kPa
Stress dependency coefficient, (m)	0.5	-
Peak shear strain, (γ)	0.10	-
Cohesion, (c)	0.1	kPa
Peak friction angle, (φ)	35.5	Degrees
Phase transformation angle, (φ_{PT})	26	Degrees
Permeability, (k)	3.0E-5	m/s
Contraction parameter, (c_1)	0.055	-
Contraction parameter, (c_2)	5	-
Contraction parameter, (c_3)	0.06	-
Dilation parameter, (d_1)	0.02	-
Dilation parameter, (d_2)	3	-
Dilation parameter, (d_3)	0.06	-
Number of yield surface	30	-

3.3.2 Parameter selection for interface element

Within the OpenSeesPL framework, the soil-pile interface was modelled using continuum interface layer elements with the PDMY02 constitutive model.

During the single element simulation, the dilation and contraction rules of the constitutive model were intentionally deactivated by assigning zero values, and the interface response was represented primarily through shear strength and deformation parameters.

The numerical simulation was conducted based on the monotonic direct shear test data reported by Zhang et al. (2021) on sand-steel specimens tested at two relative densities (D_r=30% and D_r=90%). Since, no test data were available for D_r=64%, a simplified interpolation approach was adopted. For a given effective stress level, shear responses orresponding to D_r=30% and D_r=90% were considered as lower and upper bounds. At each shear displacement level, the shear stress corresponding to D_r=64% was estimated by linear interpolation between the measured values at D_r=30% and D_r=90%. This resulted in an interpolated shear stress-displacement curve representative of the relative density of the sand used in the model test.

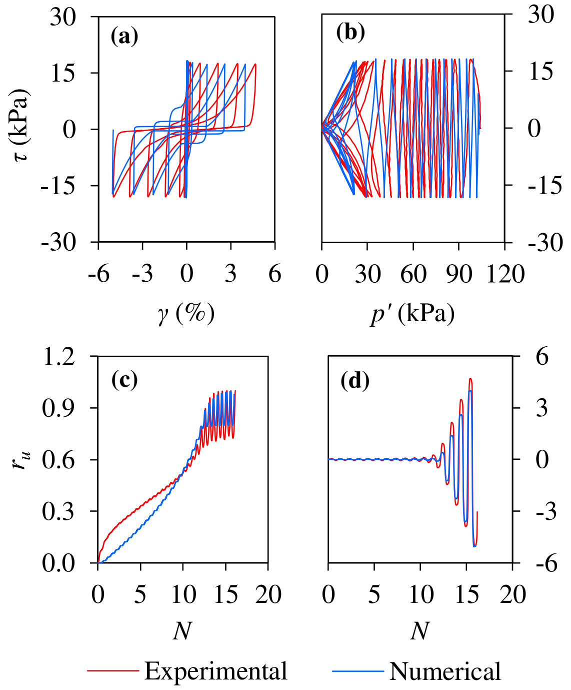

Figure 3. Comparison of experimental and single element simulation under CDSS: (a) shear stress-shear strain response, (b) effective stress path, (c) excess pore water pressure ratio and (d) shear strain over the number of loading cycles.

Figure 4 presents the experimental shear stress-shear displacement relationship together with the interpolated response obtained for D_r=64%. The selected interface model parameters are summarized in Table 5.

Table 5. Selected constitutive model parameters for interface element.

Parameter	Value	Unit
Small strain shear modulus, (G)	2.87	MPa
Small strain bulk modulus, (K)	6.23	MPa
Reference pressure, (σ'_{ref})	100	kPa
Stress dependency coefficient, (m)	0.5	-
Peak shear strain, (γ)	0.10	-
Cohesion, (c)	0.1	kPa
Peak friction angle, (φ)	22	Degrees
Phase transformation angle, (φ_{PT})	22	Degrees
Permeability, (k)	3.0E-5	m/s
Contraction parameters, (c_1,c_2,c_3)	0	-
Dilation parameters, (d_1,d_2,d_3)	0	-
Number of yield surface	30	-

It should be noted that the finite element model adopted for the interface single-element simulation is identical to that used in the single-element simulation of the soil element. Based on these modelling considerations and selected model parameters, the resulting interface response is presented in Figure 5.

The observed agreement between numerical and experimental results indicates that the adopted parameter set provides a reasonable representation of the interface behaviour within the scope of the present modelling framework. Accordingly, the selected constitutive model parameters are considered suitable for the numerical validation of the model test conducted in this study.

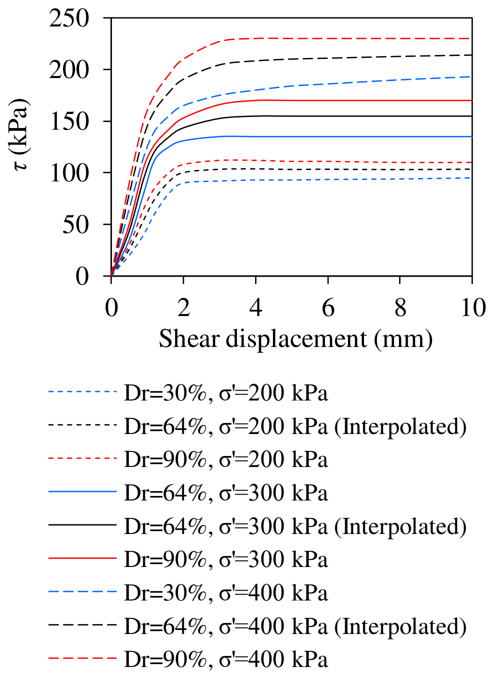

Figure 4. Monotonic direct shear test results for sand-steel interface, including interpolated values for D_r=64% (reproduced from Zhang et al., 2021).

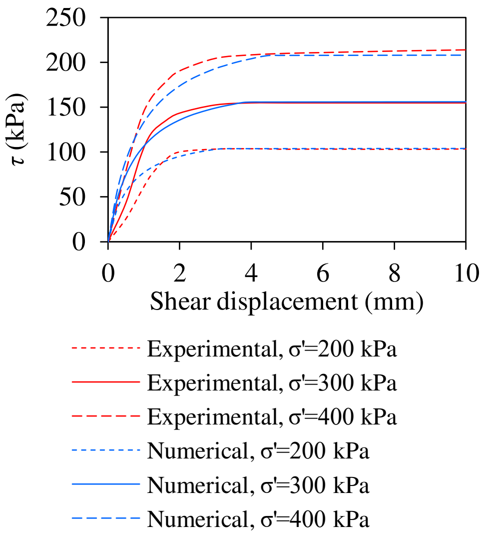

Figure 5. Experimental and numerical responses for the sand-steel interface.

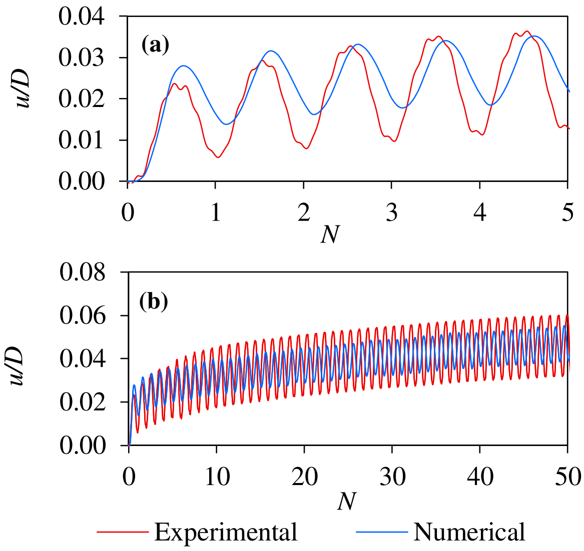

Figure 6. Normalized pile head displacements up to 5th and 50th loading cycle.

4 RESULTS

This section presents the numerical results obtained from the finite element analyses conducted in OpenSeesPL. The model was subjected to the same loading protocol applied in the physical model tests, and the simulations were performed up to 50 loading cycles.

4.1 Pile deformations and rotations

During the first loading cycle, the numerical and experimental results exhibit close agreement in terms of normalized pile head lateral displacement (u/D), particularly during the initial half-cycle. In the subsequent two cycles, the numerical model predicts slightly larger displacement amplitudes compared to the experimental results. However, from approximately the fourth cycle onwards, the computed displacements remain below the measured values. This behaviour may be attributed to the implemented interface representation and its influence on pile stiffness under cyclic behaviour.

When the overall response is considered, the mean pile head displacement over the first 50 loading cycles follows a similar trend in both the numerical and experimental results. Although differences are observed in the minimum and maximum displacement values within individual cycles, the general consistency of the cyclic response indicates that the developed model captures the principal features of the observed behaviour. Pile head displacements from both experimental and numerical studies given in Figure 6.

The distribution of lateral displacement and rotation along the pile was examined to evaluate the lateral response. In the experimental study, measurements along the pile profile were available for the 1st and 40th loading, considering first 50 loading cycle, and the corresponding numerical results are presented for comparison in Figure 7 and Figure 8.

In the figures, the depth coordinate is expressed as z/L_e, where z is measured from the pile head and L_e denotes the embedded length. Since the pile extends 0.25m above the ground surface, the total pile length (3.45m) exceeds the embedded length (3.20m). Consequently, normalization by L_e results in z/L_e values slightly greater than 1.00 near the pile tip (z/L_e=1.08).

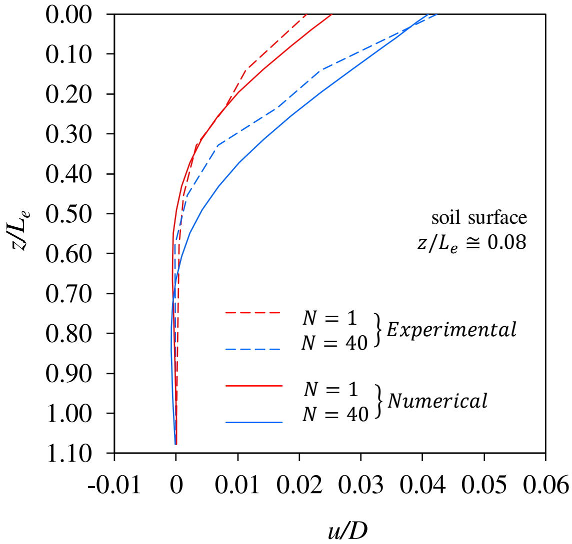

Figure 7. Normalized lateral pile displacement profiles for 1st and 40th loading cycles.

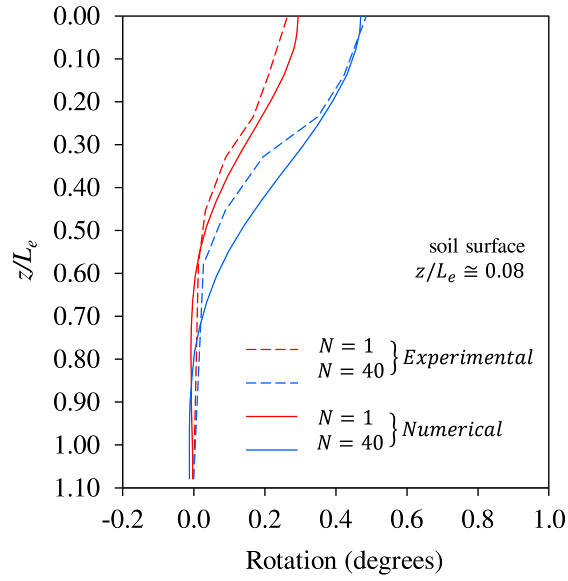

Figure 8. Rotation profiles for 1st and 40th loading cycles.

At the first loading cycle, the numerical displacement profile follows the experimental measurements, although lateral displacements are slightly overestimated in the near-head region ($0.0 \leq z/L_e \leq 0.2$), with differences reaching approximately 25%. At the 40th cycle, good agreement is obtained in the uppermost and lowermost portions of the pile, while the intermediate depths show overestimation of about 20%. A similar pattern is observed in the rotation profiles. During the first cycle, rotations are slightly overestimated in the upper part of the pile ($0 \leq z/L_e \leq 0.6$). At the 40th cycle, good agreement is obtained within $0 \leq z/L_e \leq 0.3$ and $0.7 \leq z/L_e \leq 1.1$, while overestimation remains in the intermediate region.

4.2 Soil-pile interaction

Within the scope of this study, the p-y relationships, which constitute one of the key component of soil-pile interaction, were comprehensively evaluated. The p-y curves were extracted at normalized depths of z/L_e= 0.10, 0.20 and 0.30 along the pile depth and were compared with the API (2014) recommended p-y backbone curves for sand, as illustrated in
Figure 9.

At z/L_e=0.10, the numerical response exhibits slightly stiffer behaviour during approximately the first 10 loading cycles compared to the API backbone curve. However, in the subsequent cycles, the overall response becomes softer. For the same lateral displacement level, the soil reaction (p) obtained from the numerical analysis is approximately 20-25% lower. At greater depths (z/L_e=0.20 and 0.30), the difference becomes more pronounced, with soil reactions from the API backbone curve nearly 50% higher than those from the numerical analysis. Moreover, at z/L_e=0.20, a noticeable degradation in the computed soil reaction is observed with increasing loading cycles, indicating a cycle-dependent reduction in soil resistance.

These results indicate that, under the model-scale conditions considered, the API p-y curves tend to predict higher soil reactions at intermediate depths and do not capture the cyclic reduction in soil reaction observed in the numerical simulations.

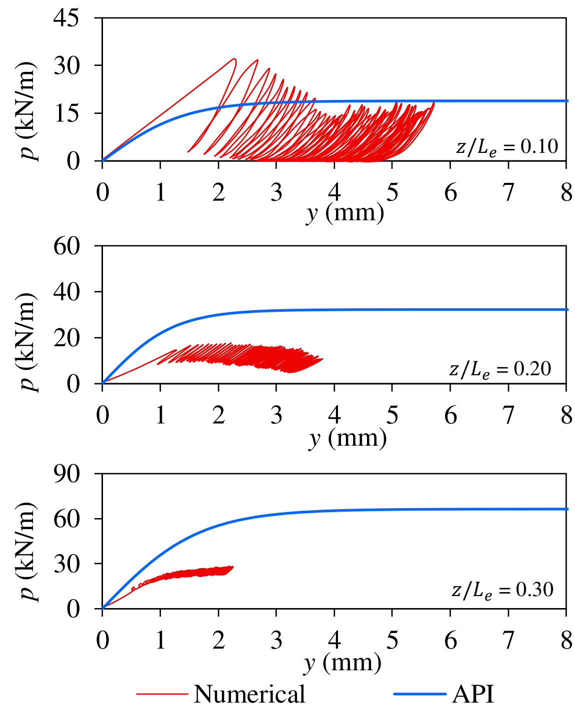

Figure 9. P-y relationship at different depths obtained from numerical study and recommended by API (2014).

5 CONCLUSIONS

This study presented a three-dimensional FEM approach for simulating the cyclic lateral response of a model-scale monopile foundation installed in saturated medium-dense sand. The numerical model developed in OpenSeesPL, employing the PDMY02 constitutive model together was validated against the 1g physical model tests reported by Akdag et al. (2023). The comparison demonstrated that the adopted modelling approach is capable of reproducing the principal characteristics of the observed behaviour during the first 50 loading cycles.

The evaluation of soil-pile interaction through computed p-y relationships indicated that the API (2014) backbone curves provide a reasonable representation of soil reaction near the ground surface under the considered model-scale conditions. However, at intermediate depths, the API curves predict higher soil reactions and do not capture the cycle-dependent reduction in soil resistance observed in the numerical simulations. These findings underline the importance of advanced numerical modelling approaches in capturing cyclic stiffness change and redistribution of soil reaction along the pile.

It should be emphasized that the proposed modelling framework is validated for the specific model-scale configuration, relative density and loading protocol considered in this study. The adopted constitutive parameters, interface thickness, and mesh configuration are therefore applicable within this validation context and should not be directly extrapolated to different soil conditions or prototype-scale applications without additional verification.

For future studies, dedicated cyclic laboratory testing on Cottbuser sand should be conducted to enable more comprehensive constitutive parameter calibration. In addition, systematic sensitivity analyses considering mesh density, interface thickness, and constitutive parameter variations are recommended to further evaluate and improve the robustness of the proposed modelling approach. Extension of the framework to prototype-scale monopile configurations under different loading scenarios is also suggested to enhance its broader applicability.

REFERENCES

Abadie, C. N., Byrne, B. W., & Houlsby, G. T. (2019). Rigid pile response to cyclic lateral loading: Laboratory tests. *Géotechnique, 69*(10), 863-876. https://doi.org/10.1680/jgeot.16.P.325

Akdag, C. T., & Rackwitz, F. (2023). Model test and finite element analysis results of a monopile in very dense sand under unidirectional horizontal cyclic loading. *Ocean Engineering*, *288*, 116053. https://doi.org/10.1016/j.oceaneng.2023.116053

Akdag, C.T., Isik, N., Le, V.H., and Rackwitz, F., (2023). Test results for a monopile in medium dense sand subjected to unidirectional lateral cyclic loading. *European Journal of Environmental and Civil Engineering*, 27(5), 1957-1988. https://doi.org/10.1080/19648189.2022.2107576

American Petroleum Institute (API). (2014). *Geotechnical and foundation design considerations*. American Petroleum Institute

Corciulo, S., Zanoli, O., & Pisano, F. (2017). Transient response of offshore wind turbines on monopiles in sand: role of cyclic hydro-mechanical soil behaviour. *Computers and geotechnics*, *83*, 221-238.

Davisson, M. T. (1970). Lateral load capacity of piles. In *Proceedings of the 49th Annual Meeting of the Highway Research Board* (pp. 104-112). Washington, DC.

El Ghoraiby, M., Park, H., & Manzari, M. T. (2019). Physical and mechanical properties of Ottawa F65 sand. In *Model tests and numerical simulations of liquefaction and lateral spreading: LEAP-UCD-2017* (pp. 45-67). Cham: Springer International Publishing. https://doi.org/10.1007/978-3-030-22818-7_3

Elgamal, A., Yang, Z., and Parra, E., (2002). Computational modeling of cyclic mobility and post-liquefaction site response. *J. Soil Dynamics and Earthquake Engineering,* Vol. 22, 259-271.

Kementzetzidis, E., Corciulo, S., Versteijlen, W. G., & Pisano, F. (2019). Geotechnical aspects of offshore wind turbine dynamics from 3D non-linear soil-structure simulations. *Soil Dynamics and Earthquake Engineering*, *120*, 181-199.

Khosravifar, A. (2012). *Analysis and design for inelastic structural response of extended pile shaft foundations in laterally spreading ground during earthquakes* (Doctoral dissertation, University of California, Davis).

Lin, S.-S., & Liao, J. C. (1999). Permanent strains of piles in sand due to cyclic lateral loads. *Journal of Geotechnical and Geoenvironmental Engineering*, 125(9), 798-802. https://doi.org/10.1061/(ASCE)1090-0241(1999)125:9(798)

Long, J. H., & Vanneste, G. (1994). Effects of cyclic lateral loads on piles in sand. *Journal of Geotechnical Engineering*, 120(1), 225-243. https://doi.org/10.1061/(ASCE)0733-9410(1994)120:1(225)

Lu, J., Elgamal, A., and Yang, Z. (2011). OpenSeesPL: 3D lateral pile-ground interaction user manual (Beta 1.0). *Department of Structural Engineering, University of California, San Diego,* 147.

Mazzoni, S., Mckenna, F., Scott, M.H., and Fenves, G.L. (2006), OpenSees command language manual, Pacific Earthquake Engineering Research Center: California.

Poulos, H. G. (1982). Single pile response to cyclic lateral load. *Journal of the Geotechnical Engineering Division, 108*(3), 355-375. https://doi.org/10.1061/AJGEB6.0001255

Vargas, R. R., Ueda, K., and Uemura, K. (2024). Dynamic torsional shear tests of Ottawa F-65 sand for LEAP-ASIA-2019. In *Model tests and numerical simulations of liquefaction and lateral spreading II: LEAP-ASIA-2019*. Springer. https://doi.org/10.1007/978-3-031-48821-4_4

Verdure, L., Garnier, J., & Levacher, D. (2003). Lateral cyclic loading of piles in sand. *International Journal of Physical Modelling in Geotechnics*, 3(3), 17-28.

Yang, Z., Elgamal, A., and Parra, E., (2003). Computational model for cyclic mobility and associated shear deformation. *J. Geotech. Geoenviron. Eng,* 129, 12, 1119-1127.

Zhang, P., Ding, S., and Fei, K. (2021). Research on shear behavior of sand-structure interface based on monotonic and cyclic tests. *Applied Sciences*, *11*(24), 11837. https://doi.org/10.3390/app112411837